EDGE ARTICLE

Check for updates

Ba₄Bi₂(Si₈−ₓB₄₊ₓO₂₉) (x = 0.09): a new acentric metal borosilicate as a promising nonlinear optical material†‡

Ru-Ling Tang,[abc] Chun-Li Hu,[a] Fei-Fei Mao,[a] Jiang-He Feng[a] and Jiang-Gao Mao [ID] *[a]

A new acentric metal borosilicate, namely Ba₄Bi₂(Si₈−ₓB₄₊ₓO₂₉) (x = 0.09), has been synthesized by a standard solid-state reaction. The title compound crystallizes in noncentrosymmetric (NCS) space group I$\bar{4}$2m with lattice parameters a = 11.0254(4) Å and c = 10.3961(9) Å. Structure refinements indicate that mixing of B atoms and Si atoms exists for a few atomic sites. In the "ideal" Ba₄Bi₂(Si₈B₄O₂₉), BO₄ or SiO₄ tetrahedra are inter-connected by corner-sharing to cyclic B₄O₁₂ or Si₄O₁₂ units. These B₄O₁₂ and Si₄O₁₂ units are further interconnected *via* corner-sharing to an "ideal" [Si₈B₄O₂₉]¹⁴⁻ 3D network. The Ba²⁺ and Bi³⁺ act as the counter cations and are located at the cavities of the structure. Ba₄Bi₂(Si₈−ₓB₄₊ₓO₂₉) (x = 0.09) melts incongruently at a high temperature of 929 °C. Powder second-harmonic generation (SHG) measurements reveal that Ba₄Bi₂(Si₈−ₓB₄₊ₓO₂₉) (x = 0.09) is a type I phase-matching compound with a good SHG response of about 5.1 times that of KDP (KH₂PO₄), which is the highest among the borosilicates reported so far. The SHG source has been studied by DFT theoretical calculations. Our preliminary results indicate that Ba₄Bi₂(Si₈−ₓB₄₊ₓO₂₉) (x = 0.09) is a new second-order nonlinear-optical crystalline material candidate.

Introduction

Noncentrosymmetric solid materials have always been an active research field due to their unique physical performances, such as second-order nonlinear optics (NLO), piezoelectricity, pyroelectricity, ferroelectricity, *etc.*[1–9] In the second-harmonic generation domain particularly, a variety of excellent acentric materials have been synthesized including the famous NLO materials, such as β-BaB₂O₄ (β-BBO) and LiB₃O₅ (LBO).[10,11] Recently, fluorooxoborates have aroused great interest due to their short ultraviolet cutoff edge. Some new acentric fluorooxoborates have been discovered, such as AB₄O₆F (A = NH₄, Na, K, Rb, or Cs).[12–16]

As for the NLO materials used in the deep-ultraviolet (DUV) region, the KBe₂BO₃F₂ (KBBF) crystal is the only material that can produce coherent light wavelengths below 200 nm by direct SHG.[17,18] After continuous efforts, a number of new beryllium borate crystals of the KBBF family have been discovered including β-KBe₂B₃O₇, γ-KBe₂B₃O₇, RbBe₂B₃O₇, Na₂Be₄B₄O₁₁ and LiNa₅Be₁₂B₁₂O₃₃.[19–21] Unfortunately, due to the weak interlayer bonding force and the toxicity of Be²⁺ in these materials, their crystal growth and wide industrial applications are still restricted. Hence, finding an appropriate composition to substitute beryllium has aroused widespread research interest.

Considering the coordination environment of beryllium atoms, a very effective strategy is to replace BeO₄ tetrahedra with PO₄, SiO₄ and GeO₄, which led to the formation of a variety of metal borophosphates, borogermanates and borosilicates, including Ba₃(ZnB₅O₁₀)PO₄, Na₄MB₂P₃O₁₃ (M = Rb, Cs), A₂EB₄O₉ (A = Cs, Rb) (E = Si, Ge), AEB₃O₇ (A = Cs, Rb) (E = Si, Ge), and Ba₄(BO₃)₃(SiO₄)·Ba₃X (X = Cl, Br).[22–29] Recently, the partial disorder between Ge atoms and B atoms in tetrahedral positions has led to borogermanates with interesting structures, as shown by CsBₓGe₆−ₓO₁₂ (x = 1) and Sr₃−ₓ/₂B₂−ₓGe₄₊ₓO₁₄ (x = 0.32).[30,31]

A₂EB₄O₉ (A = Cs, Rb) (E = Si, Ge) and AEB₃O₇ (A = Cs, Rb) (E = Si, Ge) possess relatively large SHG responses in inorganic metal borogermanate and borosilicate systems; for example, Cs₂GeB₄O₉ has a SHG response of 2.8 × KDP and Cs₂SiB₄O₉ exhibits a SHG response of 4.6 × KDP.[24,27] A₂EB₄O₉ (A = Cs, Rb) (E = Si, Ge) features a three-dimensional anionic open framework formed by corner-sharing EO₄ tetrahedra and B₄O₉ clusters, with A⁺ cations filling in the anionic channels formed by

[a] State Key Laboratory of Structural Chemistry, Fujian Institute of Research on the Structure of Matter, Chinese Academy of Sciences, Fuzhou 350002, P. R. China. E-mail: mjg@fjirsm.ac.cn

[b] School of Physical Science and Technology, ShanghaiTech University, Shanghai 201210, China

[c] University of the Chinese Academy of Sciences, Beijing, 100049, China

† Dedicated to Prof. Jin-Shun Huang on the occasion of his 80th birthday.

‡ Electronic supplementary information (ESI) available. CCDC 1864258. For ESI and crystallographic data in CIF or other electronic format see DOI: 10.1039/c8sc04342f

nine-/ten-membered rings. It is noticed that alkaline-earth metal borogermanates and borosilicates display a relatively weaker SHG response, for example, $Ba_4(BO_3)_3(SiO_4) \cdot Ba_3X$ (X = Cl, Br) (1 × KDP) and $Ba_3[Ge_2B_7O_{16}(OH)_2](OH)(H_2O)$ (0.3 × KDP).[32,33]

Compared with metal borates and fluorooxoborates, it is obvious that the SHG responses of most acentric borosilicates and borogermanates are relatively weak. To increase their SHG responses, one useful method is to introduce SHG active cations with stereo-active lone pairs, such as Pb^{2+}, Sn^{2+}, and Bi^{3+}.[34–36]

We have been trying to introduce cations with lone pairs into metal borogermanates and borosilicates to obtain materials with enhanced SHG performance. In this work, we have successfully synthesized $Ba_4Bi_2(Si_{8-x}B_{4+x}O_{29})$ ($x = 0.09$) (BBSBO) by solid state reactions. It exhibits an SHG response of 5.1 × KDP. In this compound, mixing of B atoms and Si atoms for some atomic sites occurred, which is similar to what was observed for a few borogermanates previously reported.[30,31] In this work, the synthesis, crystal structure, second-order nonlinear-optical effects, and thermal stability of this compound are reported.

Results and discussion

The title compound crystallizes in noncentrosymmetric space group $I\bar{4}2m$ (no. 121) with lattice parameters of $a = 11.034(3)$ Å and $c = 10.410(6)$ Å (Table S1‡). The asymmetric unit of this compound contains two B^{3+}/Si^{4+} mixed sites, one Bi atom, one Ba atom, and five O atoms. The first one at a 16j site is mainly Si^{4+} (92.6%) mixed with a small amount of B^{3+} (7.4%), whereas the one at the 8g site is mainly B^{3+} (87.5%) mixed with 12.5% of Si^{4+}. All of the Si^{4+} and B^{3+} atoms are tetrahedrally connected with four oxygen atoms. The M1 position based on mainly Si atoms showed M−O distances from 1.584 Å to 1.619 Å. Four $M(1)O_4$ tetrahedra form a cyclic $M(1)_4O_{12}$ unit (Fig. 2a). The $M(2)O_4$ tetrahedral centers based on mainly B atoms also form similar $M(2)_4O_{12}$ units (Fig. 2b), and the M−O distances are within the range from 1.490 Å to 1.509 Å. Each $M(1)_4O_{12}$ unit is corner-shared with four $M(2)_4O_{12}$ units (Fig. 2c), while each

$M(2)_4O_{12}$ unit is corner-shared with eight $M(1)_4O_{12}$ units (Fig. 2d). Such connectivity led to a 3D anionic framework (Fig. 1b). The Ba^{2+} atom is ten-coordinated with Ba–O distances ranging from 2.734(5) to 3.2092(4) Å (Fig. 2f). Coordinated with five oxygen atoms, the Bi^{3+} atoms are in a BiO_5 square pyramidal geometry with four Bi–O1 (2.327(3) Å) and one Bi–O5 (2.0748(3) Å) (Fig. 2e). The unpaired electrons of the Bi^{3+} ion are oriented towards the open side of the BiO_4 square (opposite to O5). All the Ba^{2+} and Bi^{3+} act as the counter cations and are filled in the tunnels of the 8-member rings of the anionic framework (Fig. 1a).

The anionic borosilicate framework in $LnBSiO_5$ (Ln = La, Ce, Nd) is also solely composed of BO_4 and SiO_4 tetrahedral groups.[37] However, the BO_4 and SiO_4 arrange in a different way. In $LnBSiO_5$, the BO_4 tetrahedra form infinite helical chains with the SiO_4 tetrahedra grafting on the 1D chain by bridging with two neighboring BO_4 tetrahedra, hence forming 1D borosilicate chains based on B_2Si three-membered rings.

About the site-mixing of B and Si atoms, it is not very common in the borosilicates reported. However two borogermanates, namely, $CsB_xGe_{6-x}O_{12}$ ($x = 1$) (CBGO) and $Sr_{3-x/2}B_{2-x}Ge_{4+x}O_{14}$ ($x = 0.32$) (SBGO), have been reported to exhibit the mixing of the B and Ge atoms at the same site.[30,31] There is only one mixed occupied site of B^{3+}/Ge^{4+} in the structure of CBGO, and it has the percentage of B^{3+} (16.6%) and Ge^{4+} (83.3%). B/GeO_4 tetrahedra are interconnected leading to an octahedral cage, and each connects with the eight nearest ones (Fig. 3a). Cs^+ acts as the counter cation located in each cage, which produces a zeolite SOD-type net.[30] As for SBGO, it exhibits a $Ca_3Ga_2Ge_4O_{14}$-like structure (Fig. 3b). SBGO exhibits both GeO_4 tetrahedra and GeO_6 octahedra. The mixed Ge^{4+}/B^{3+} site is tetrahedrally coordinated with Ge^{4+} (16%) and B^{3+} (84%). The B/GeO_4 tetrahedron connects with three other GeO_4 tetrahedra by sharing three corners in a layered structure.[31] We deem that the mixing of B and Si atoms at the same site should be more likely compared with the B/Ge mixing due to being closer in size; hence we believe that more similar examples will be found in the future.

The TG and DSC curves are given in Fig. S4.‡ The thermal behavior of BBSBO is measured from 30 to 1000 °C. The TG
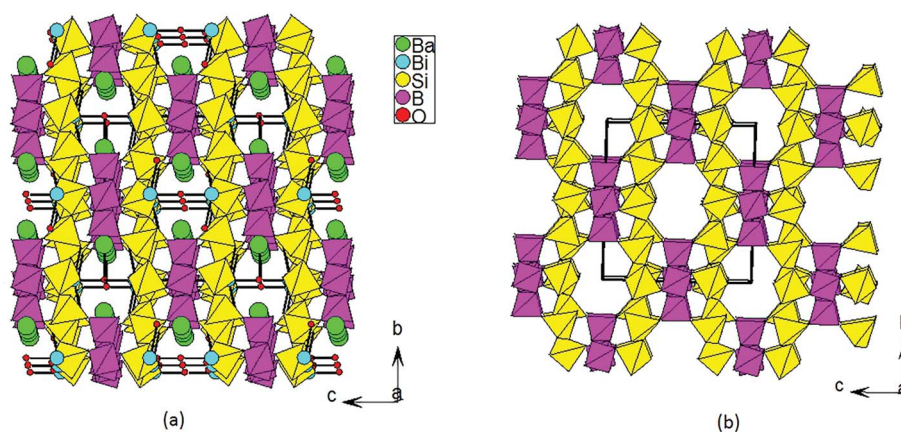

Fig. 1 View of the 3D crystal structure of BBSBO down the a axis (a); view of the 3D anionic framework of BBSBO with tunnels of 8-MRs along the a axis (b).
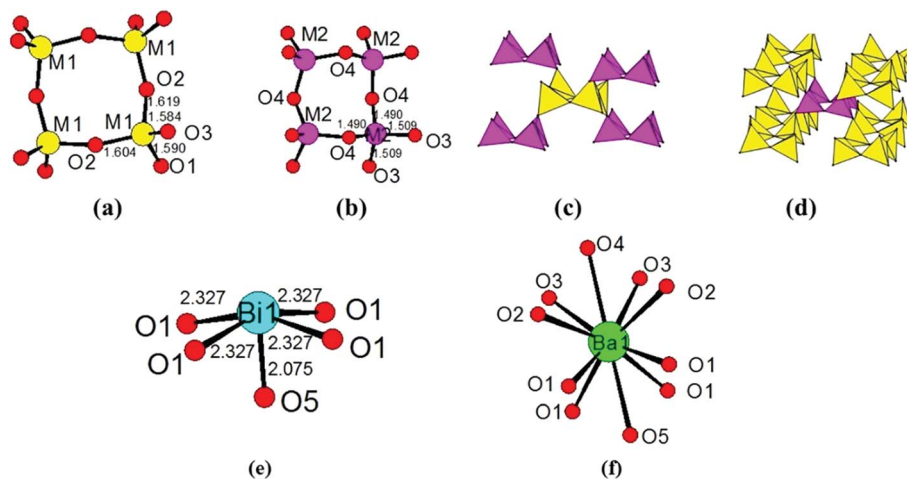
Fig. 2 An $M(1)_4O_{12}$ unit (a); an $M(2)_4O_{12}$ unit (b); an $M(1)_4O_{12}$ unit corner-sharing with four $M(2)_4O_{12}$ units (c); an $M(2)_4O_{12}$ unit corner-sharing with eight $M(1)_4O_{12}$ (d); the coordination environment of the Bi atom (e); and the coordination environment around the Ba atom (f).
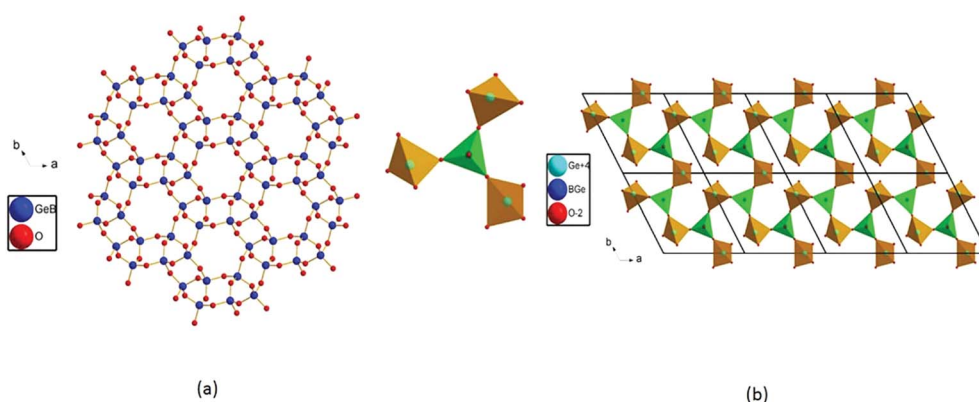

Fig. 3 The Ge/BO_4 tetrahedral cage in $CsB_xGe_{6-x}O_{12}$ ($x = 1$) (a); the B/GeO_4–GeO_4 layer in $Sr_{3-x/2}B_{2-x}Ge_{4+x}O_{14}$ ($x = 0.32$) (b).

results show that there is no apparent weight loss before 1000 °C, which indicates that this compound has very high thermal stability. As shown in the graph, there is one clear endothermic peak at 929 °C but no exothermic peak in the cooling curves, which indicates that this compound melts incongruently. The peak at 929 °C is later proved to be the melting point. The powder XRD pattern for the sample heated at 940 °C does not match the calculated PXRD (Fig. S1‡); hence the material goes through incongruent melting. Through phase analysis, the residuals are mainly $Ba_{0.5}Bi_{1.5}O_{2.16}$, SiO_2 and B_2O_3.

The UV-Vis absorption spectrum of BBSBO is displayed in Fig. S3.‡ It is shown that the UV cutoff edge of BBSBO is 318 nm. The UV spectrum indicates that the band gap of BBSBO is 3.89 eV (Fig. S3‡). Strong absorption bands are observed with vibration frequencies within 1100 cm^{-1} in the IR spectrum of BBSBO (Fig. S2‡). According to ref. 38, the high-frequency peaks located at 1100 to 740 cm^{-1} are well matched with the BO_4^{5-} and SiO_4^{4-} unit stretching vibrations. The BO_4 and SiO_4 group bending vibration bands should be below 660 cm^{-1} in the figure. Due to some overlap of vibration bands for BO_4 and SiO_4

groups, these absorption bands cannot be assigned undoubtedly, which is common in the reported ref. 34 and 39.

Powder SHG signals of BBSBO crystals at a wavelength of 1064 nm are exhibited in Fig. 4. Comparing the SHG intensity
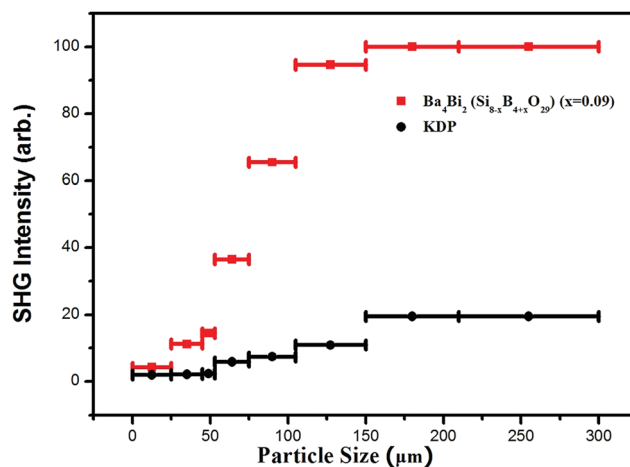

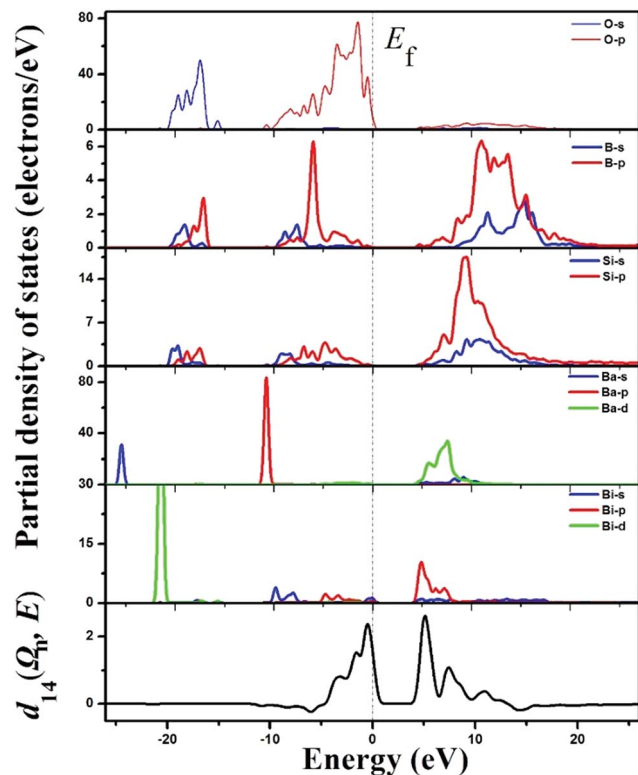**Fig. 4** SHG measurements of BBSBO.

Fig. 5 The partial density of states (the upper five panels) and the spectral decomposition of d_{14} (the bottommost panel) for BBSBO.

produced by BBSBO and KDP shows that BBSBO has a good SHG effect of 5.1 × KDP, which is the largest among metal borosilicates reported to date, and BBSBO is phase-matching based on the rule established by Kurtz and Perry.[40] The SHG source of the title compound may have originated from the synergistic effect of Bi^{3+}, BO_4 and SiO_4 groups.

To learn about the SHG response origin of BBSBO more deeply, theoretical computations on an ideal "$Ba_4Bi_2(Si_8B_4O_{29})$" structure were made based on DFT methods. The band

structure calculations reveal that BBSBO is an indirect band-gap material (from Z to G) (Fig. S5 and Table S5‡). The theoretical band gap is 4.35 eV, being larger than the value of 3.89 eV obtained by experimental measurement. The result is not unreasonable, because it is common that GGA cannot precisely depict the eigenvalues of the conduction bands.[41–44]

From the upper five panels in the partial density of states (PDOS) graph of BBSBO (Fig. 5), the bands and the bonding interactions of the structure can be easily assigned and understood. We study the vicinity of the Fermi level from −10 to 8 eV to account for the bonding trait and optical properties of BBSBO. Obviously, the electronic states of Si and B atoms are well overlapped with coordinated O atoms, signifying the firm bonding interactions. Similarly, Bi atoms are greatly overlapped with the O atoms in some regions too. The upper region of the VB from −5.0 to 0 eV is mainly the 2p nonbonding states of oxygen atoms. Particularly, a few of the flat bands at the top of the VB are ascribed to the nonbonding states of oxygen atoms that are bonded to Bi and some of the Bi-6s states; in addition, the bottommost part of the CB originates from the unoccupied Bi-6p and some O-2p states bonded to Bi. Hence the band gap of BBSBO rests with BiO_5 anionic groups.

We further calculated the second-order nonlinear optical properties of BBSBO. BBSBO crystallized in $I\bar{4}2m$ space group, which belongs to the point group $\bar{4}2m$ and has only one nonzero SHG tensor (d_{14}) in consideration of Kleinman symmetry. The calculated SHG tensor $d_{14} = 5.20 \times 10^{-9}$ esu coincides with the experimental value of 5.1 times that of KDP.

Moreover, we analyzed the SHG source of BBSBO. We performed the spectral decomposition and the SHG density analyses of tensor d_{14}. It is obvious that the upper part of the VB (−5.0–0 eV) and the lower part of the CB (<10 eV) are the most SHG-active energy regions of d_{14} (Fig. 5), corresponding to O-2p electronic states in the VB and unoccupied Bi-6p, Ba-5d, Si-3p, B-2p, and O-2p in the CB. It is worth noting that the SHG density of d_{14} (Fig. 6) indicates that the 2p nonbonding states of all O atoms in the VB make a prominent difference to the SHG
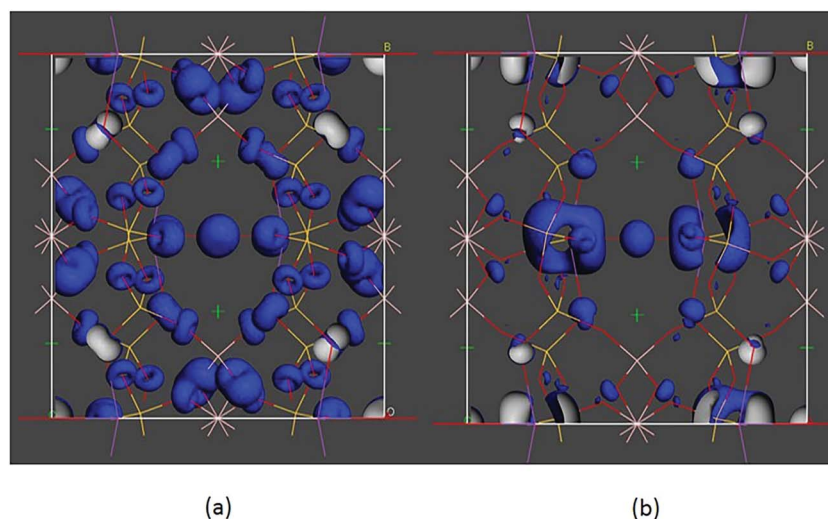

Fig. 6 The SHG density of d_{14} in the VB (a) and CB of BBSBO (b).

effect, while the unoccupied Bi-6p and some O-2p orbitals contribute the most to the SHG process in the CB. By calculating the SHG density in amount, the SHG contribution percentages of BBSBO are 27.70%, 34.47%, 19.95% and 17.88% for BiO_5, SiO_4, BO_4 and Ba^{2+}, respectively. Notably, all anionic groups work well in the SHG process. It's also worth noting that as counter-ions, the Ba^{2+} cations contribute a lot to the SHG effect, which is very similar to the effect of Cs^+ in the NLO compound of $LiCs_2PO_4$.[45] Therefore, the synergistic effect of all the groups/ions makes BBSBO a remarkable SHG crystal.

Conclusions

In summary, a new acentric borosilicate, $Ba_4Bi_2(Si_{8-x}B_{4+x}O_{29})$ ($x = 0.09$), has been synthesized and characterized. For the first time, Bi^{3+} has been introduced into the borosilicate system. BBSBO exhibits a strong SHG response which is 5.1 times that of KDP (KH_2PO_4) and possesses high thermal stability. According to first-principles calculations, the synergistic effect of Bi^{3+} and Ba^{2+} and SiO_4 and BO_4 groups led to an outstanding SHG response of the title compound. Our achievement in the case of BBSBO provides a feasible strategy for designing novel borosilicates and borogermanates with excellent SHG performance. Our future research efforts will be committed to the exploration of other borosilicates or borogermanates containing lone pair cations or fluoride anions.

Conflicts of interest

The authors declare no competing financial interests.

Acknowledgements

Notes and references

1 H. Yu, J. Young, H. Wu, W. Zhang, J. M. Rondinelli and P. S. Halasyamani, *Chem. Mater.*, 2017, **29**, 1845–1855.

2 P. Kumar and A. Gaur, *Ceram. Int.*, 2017, **43**, 16403–16407.

3 H. Yu, W. Zhang, J. Young, J. M. Rondinelli and P. S. Halasyamani, *J. Am. Chem. Soc.*, 2016, **138**, 88–91.

4 J. Dalal and B. Kumar, *Opt. Mater.*, 2016, **51**, 139–147.

5 K. Lin, Z. Zhou, L. Liu, H. Ma, J. Chen, J. Deng, J. Sun, L. You, H. Kasai, K. Kato, M. Takata and X. Xing, *J. Am. Chem. Soc.*, 2015, **137**, 13468–13471.

6 C. M. N. Kumar, Y. Xiao, P. Lunkenheimer, A. Loidl and M. Ohl, *Phys. Rev. B: Condens. Matter Mater. Phys.*, 2015, **91**, 235149.

7 G. Zhang, Y. J. Li, K. Jiang, H. Y. Zeng, T. Liu, X. G. Chen, J. G. Qin, Z. S. Lin, P. Z. Fu, Y. C. Wu and C. T. Chen, *J. Am. Chem. Soc.*, 2012, **134**, 14818–14822.

8 K. M. Ok, E. O. Chi and P. S. Halasyamani, *Chem. Soc. Rev.*, 2006, **35**, 710–717.

9 P. Becker, *Adv. Mater.*, 1998, **10**, 979–992.

10 C. T. Chen, B. C. Wu, A. D. Jiang and G. M. You, *Sci. Sin., Ser. B*, 1985, **589**, 235–243.

11 C. T. Chen, Y. C. Wu, A. D. Jiang, G. M. You, R. K. Li and S. J. Lin, *J. Opt. Soc. Am. B*, 1989, **6**, 616–621.

12 Z. Zhang, Y. Wang, B. Zhang, Z. Yang and S. Pan, *Angew. Chem., Int. Ed.*, 2018, **57**, 1–6.

13 G. Shi, Y. Wang, F. Zhang, B. Zhang, Z. Yang, X. Hou, S. Pan and K. R. Poeppelmeier, *J. Am. Chem. Soc.*, 2017, **139**, 10645–10648.

14 Y. Wang, B. Zhang, Z. Yang and S. Pan, *Angew. Chem., Int. Ed.*, 2018, **57**, 2150–2154.

15 M. Mutailipu, M. Zhang, H. Wu, Z. Yang, Y. Shen, J. Sun and S. Pan, *Nat. Commun.*, 2018, **9**, 3089.

16 M. Mutailipu, M. Zhang, B. Zhang, L. Wang, Z. Yang, X. Zhou and S. Pan, *Angew. Chem., Int. Ed.*, 2018, **57**, 6095–6099.

17 C. Chen, Z. Xu, D. Deng, J. Zhang, G. K. L. Wong, B. Wu, N. Ye and D. Tang, *Appl. Phys. Lett.*, 1996, **68**, 2930–2932.

18 B. Wu, D. Tang, N. Ye and C. Chen, *Opt. Mater.*, 1996, **5**, 105–109.

19 S. C. Wang, N. Ye, W. Li and D. Zhao, *J. Am. Chem. Soc.*, 2010, **132**, 8779–8786.

20 X. X. Jiang, S. Y. Luo, L. Kang, P. F. Gong, H. W. Huang, S. C. Wang, Z. S. Lin and C. T. Chen, *ACS Photonics*, 2015, **2**, 1183–1191.

21 H. W. Huang, L. J. Liu, S. F. Jin, W. J. Yao, Y. H. Zhang and C. T. Chen, *J. Am. Chem. Soc.*, 2013, **135**, 18319–18322.

22 H. Yu, W. Zhang, J. Young, J. M. Rondinelli and P. S. Halasyamani, *Adv. Mater.*, 2015, **27**, 7380–7385.

23 C. Wu, L. Li, G. Yang, J. Song, B. Yan, M. G. Humphrey, L. Zhang, J. Shao and C. Zhang, *Dalton Trans.*, 2017, **46**, 12605–12611.

24 X. Xu, C. L. Hu, F. Kong, J. H. Zhang, J. G. Mao and J. Sun, *Inorg. Chem.*, 2013, **52**, 5831–5837.

25 J. H. Zhang, C. L. Hu, X. Xu, F. Kong and J. G. Mao, *Inorg. Chem.*, 2011, **50**, 1973–1982.

26 F. Kong, H. L. Jiang, T. Hu and J. G. Mao, *Inorg. Chem.*, 2008, **47**, 10611–10617.

27 H. Wu, H. Yu, S. Pan, Z. Huang, Z. Yang, X. Su and K. R. Poeppelmeier, *Angew. Chem., Int. Ed.*, 2013, **52**, 3406–3410.

28 Z. Zhou, Y. Qiu, F. Liang, L. Palatinus, M. Poupon, T. Yang, R. Cong, Z. Lin and J. Sun, *Chem. Mater.*, 2018, **30**, 2203–2207.

29 X. Lin, F. Zhang, S. Pan, H. Yu, F. Zhang, X. Dong, S. Han, L. Dong, C. Bai and Z. Wang, *J. Mater. Chem. C*, 2014, **2**, 4257–4264.

30 R. Pan, J. W. Cheng, B. F. Yang and G. Y. Yang, *Inorg. Chem.*, 2017, **56**, 2371–2374.

31 B. Petermuller, L. L. Petschnig, K. Wurst, G. Heymann and H. Huppertz, *Inorg. Chem.*, 2014, **53**, 9722–9728.

32 J. H. Zhang, F. Kong and J. G. Mao, *Inorg. Chem.*, 2011, **50**, 3037–3043.

33 X. Xu, C. L. Hu, F. Kong, J. H. Zhang and J. G. Mao, *Inorg. Chem.*, 2011, **50**, 8861–8868.

34 J. L. Song, C. L. Hu, X. Xu, F. Kong and J. G. Mao, *Angew. Chem., Int. Ed.*, 2015, **54**, 3679.

35 M. Xia, X. Jiang, Z. Lin and R. Li, *J. Am. Chem. Soc.*, 2016, **138**, 14190–14193.

36 M. Luo, F. Liang, Y. Song, D. Zhao, N. Ye and Z. Lin, *J. Am. Chem. Soc.*, 2018, **140**, 6814–6817.

37 L. Li, Q. Jing, Z. Yang, X. Su, B.-H. Lei, S. Pan, F. Zhang and J. Zhang, *J. Appl. Physiol.*, 2015, **118**, 979–992.

38 Y. Shi, J. K. Liang, H. Zhang, J. L. Yang, W. D. Zhuangv and G. H. Rao, *J. Alloys Compd.*, 1997, **259**, 163–169.

39 H. Yang, C. L. Hu, X. Xu and J. G. Mao, *Inorg. Chem.*, 2015, **54**, 7516–7523.

40 P. Kubelka and F. Z. Munk, *Tech. Phys.*, 1931, **12**, 593–601.

41 J. Zhu, W. D. Cheng, D. S. Wu, H. Zhang, Y. J. Gong and H. N. Tong, *J. Solid State Chem.*, 2006, **179**, 597–604.

42 J. Zhu, W. D. Cheng and D. S. Wu, *Eur. J. Inorg. Chem.*, 2010, **2007**, 285–290.

43 B. P. Yang, C. L. Hu, X. Xu, C. Huang and J. G. Mao, *Inorg. Chem.*, 2013, **52**, 5378–5384.

44 D. Yan, C. L. Hu and J. G. Mao, *CrystEngComm*, 2016, **18**, 1655–1664.

45 X. Y. Cheng, M. H. Whangbo, G. C. Guo, M. C. Hong and S. Q. Deng, *Angew. Chem., Int. Ed.*, 2018, **57**, 3933–3937.